

NADH can be transferred into mitochondria through the NADH shuttles, and concomitantly it leads to an increase in $[Ca^{2+}]_m$ after the formation of mitochondrial membrane potential, thereby activating pyruvate oxidation in the TCA cycle. The NADH shuttles thus would contribute to sufficient ATP generation to trigger glucose-induced insulin secretion. When NADH shuttles are halted, the activity of the TCA cycle is also decreased by ~50%, at least in part because of concurrent inhibition of Ca^{2+} entry into mitochondria. The resultant severe decrease in mitochondrial ATP synthesis to ~25% of the normal state no longer maintains glucose-induced insulin secretion (Fig. 4C). Thus, defects in the generation of mitochondrial metabolic signals through the NADH shuttles might contribute to the impairment of glucose-induced insulin secretion seen in non-insulin-dependent diabetes mellitus.

References and Notes

1. F. M. Ashcroft *et al.*, *J. Cell Biochem.* **55** (suppl.), 54 (1994); F. M. Matschinsky, *Diabetes* **45**, 223 (1996); C. B. Wollheim *et al.*, *Diabetes Rev.* **4**, 276 (1996).
2. A. Sener *et al.*, *Biochem. J.* **176**, 217 (1978); W. S. Zawulich and K. C. Zawulich, *J. Biol. Chem.* **272**, 3527 (1997).
3. I. D. Dukes *et al.*, *J. Biol. Chem.* **269**, 10979 (1994); R. J. Mertz *et al.*, *ibid.* **271**, 4838 (1996).
4. W. J. Malaisse *et al.*, *Metabolism* **28**, 373 (1979); C. J. Hedeskov *et al.*, *Biochem. J.* **241**, 161 (1987); W.-F. Pralong *et al.*, *EMBO J.* **9**, 53 (1990).
5. M. J. MacDonald, *J. Biol. Chem.* **256**, 8287 (1981).
6. _____, *Arch. Biochem. Biophys.* **213**, 643 (1982).
7. A BALB/c mouse *mGPDH* gene containing exons 4, 5, and 6 was cloned and a neomycin resistance gene under transcriptional control of the mouse phosphoglycerate kinase-1 promoter (PGK-neo) was inserted within exon 5. The 8.1 kb (5') and 1.7 kb (3') of genomic DNA flanking PGK-neo was ligated into a pMCDT-A plasmid (Gibco-BRL) that produces diphtheria toxin A fragment for negative selection. The completed targeting vector was linearized and electroporated into T12 embryonic stem cells. The cells were cultured with G418. The choice of targeted clones was based on the shift of a genomic fragment by Pvu II digestion from 3.4 to 3.1 kb, as determined by Southern (DNA) blot. Targeted embryonic stem cells were injected into blastocysts from C57BL/6j mice to sequentially obtain chimeric, heterozygous, and homozygous offspring. All the mice used were males from heterozygous breeding pairs. All islets were from 16- to 20-week-old mice.
8. W. J. Malaisse *et al.*, *Endocrinology* **111**, 392 (1982).
9. Antibody to mGPDH was raised against the COOH-terminal sequence Lys-Thr-Ala-Glu-Glu-Asn-Leu-Asp-Arg-Arg-Val-Pro-Ile-Pro-Val-Asp-Arg-Ser-Cys-Gly-Gly-Leu. Islets were isolated by collagenase digestion and homogenated in 0.23 M mannitol, 0.07 M sucrose, and 5 mM Hepes (pH 7.5). Activities of mGPDH were measured as described [R. S. Gardner, *Anal. Biochem.* **59**, 272 (1974)].
10. Relative to wild-type controls, male and female *mGPDH*^{-/-} mice at 16 weeks of age were smaller by 23% and 13%, respectively. Relative to wild-type islets, *mGPDH*^{-/-} islets had normal cellular architecture and contained approximately the same amounts of insulin and glucagon.
11. For the glucose tolerance test, glucose (1.5 mg/g body weight) was injected into the peritoneum. Blood samples were drawn from tail veins.
12. Insulin secretion was measured with Krebs-Ringer-bicarbonate buffer containing 118.4 mM NaCl, 4.7 mM KCl, 1.3 mM MgSO₄, 1.2 mM KH₂PO₄, 2.0 mM CaCl₂, 10 mM NaHCO₃, 10 mM Hepes (pH 7.4), and 0.1% bovine serum albumin at 37°C. Basal glucose concentration was 2.8 mM, and AOA was added to buffer during

preincubation (30 min) and throughout the incubation period unless otherwise stated.

13. Islet homogenates were centrifuged at 600g for 5 min and the supernatant was centrifuged at 5500g for 10 min to sediment the mitochondrial fraction. The resulting supernatant was used as the cytosolic fraction.
14. Perfusion experiments were done with 30 islets per chamber at 37°C with a flow rate of 0.6 ml/min.
15. F. Schuit *et al.*, *J. Biol. Chem.* **272**, 18572 (1997).
16. For fluorescence studies, a single islet was placed under a microscope (IMT-2; Olympus, Japan) and perfused with buffer containing 150 mM NaCl, 5 mM KCl, 1.0 mM MgCl₂, 2.0 mM CaCl₂, and 10 mM Hepes (pH 7.4) at 37°C. Fluorescence was excited with light emitted from a xenon lamp (TILL Photonics, Germany), collected through interference filters (Olympus), and detected using a photomultiplier (NTS783; Hamamatsu Photonics, Japan). NAD(P)H was measured by autofluorescence excited at 360 nm and filtered at 470 nm.
17. M. R. Duchon *et al.*, *Biochem. J.* **294**, 35 (1993).
18. For measurement of mitochondrial membrane potential, islets were loaded with Rh123 (10 µg/ml, Sigma) at 37°C for 10 min. The fluorescence was excited at 490 nm and filtered at 530 nm as described [P. Maechler *et al.*, *EMBO J.* **16**, 3833 (1997)].
19. W. J. Malaisse and A. Sener, *Biochim. Biophys. Acta* **927**, 190 (1987).
20. M. Erecinska *et al.*, *ibid.* **1101**, 273 (1992).
21. E. D. Kennedy *et al.*, *J. Clin. Invest.* **98**, 2524 (1996).
22. M. L. Litsky and D. R. Pfeiffer, *Biochemistry* **36**, 7071 (1997).

23. For measurement of $[Ca^{2+}]_m$, islets were loaded with 10 µM Rhod 2/acetoxymethylester (Molecular Probes) at 37°C for 1 hour and further incubated for 3 to 5 hours to eliminate the dye from cytosol [G. Hajnóczky *et al.*, *Cell* **82**, 415 (1995); D. R. Trollinger *et al.*, *Biochem. Biophys. Res. Commun.* **236**, 738 (1997)]. The fluorescence was excited at 480 nm and filtered at 500 nm.
24. T. E. Gunter *et al.*, *Am. J. Physiol.* **267**, C313 (1994).
25. For measurement of $[Ca^{2+}]_c$, islets were loaded with 15 µM Fura 2/acetoxymethylester (Molecular Probes) at 37°C for 1 hour. The fluorescence was excited alternately at 340 and 380 nm and filtered at 500 nm.
26. N. Hamakawa and T. Yada, *Cell Calcium* **17**, 21 (1995); F. M. Ashcroft *et al.*, *Nature* **312**, 446 (1984).
27. K. Eto *et al.*, unpublished data.
28. Results are presented as means ± SE. The significance of the differences between groups was determined using one-way analysis of variance.
29. We thank C. B. Wollheim and F. M. Ashcroft for invaluable discussion, Y. Kagawa, H. Sakura, M. Noda, and K. Yasuda for critical reading of the manuscript, and N. Takeda, M. Nagai, H. Yajima, C. Sato, H. Chiyonobu, and J. Taka for support. Supported by a grant-in-aid for creative basic research (10NP0201) from the Ministry of Education, Science, Sports, and Culture of Japan (T.K.) and by CREST of the Japan Science and Technology Corporation (H.K.).

25 August 1998; accepted 12 January 1999

Conserved Structures of Mediator and RNA Polymerase II Holoenzyme

Francisco J. Asturias,* Yi Wei Jiang, Lawrence C. Myers, Claes M. Gustafsson,† Roger D. Kornberg‡

Single particles of the mediator of transcriptional regulation (Mediator) and of RNA polymerase II holoenzyme were revealed by electron microscopy and image processing. Mediator alone appeared compact, but at high pH or in the presence of RNA polymerase II it displayed an extended conformation. Holoenzyme contained Mediator in a fully extended state, partially enveloping the globular polymerase, with points of apparent contact in the vicinity of the polymerase carboxyl-terminal domain and the DNA-binding channel. A similarity in appearance and conformational behavior of yeast and murine complexes indicates a conservation of Mediator structure among eukaryotes.

Mediator was isolated as a complex of nearly 20 proteins required to support transcriptional activation in a fully reconstituted yeast RNA polymerase II transcription system (1, 2). Mediator subunits fall into three groups: Srb proteins (3), a Sin4/Rgr1 group shown to form a distinct module that functions in repression as well as in activation (4, 5), and a group of

proteins termed "Med" for Mediator (5). A related complex, containing four homologs of yeast Mediator subunits, has been isolated from murine cells (6). Yeast and murine complexes interact with RNA polymerase II through the polymerase's COOH-terminal domain (CTD) to form a 1.5-MD holoenzyme (2, 3, 5). We report here on the structures of Mediator and the holoenzyme as seen in projection.

Yeast Mediator, resolved to homogeneity as described (7, 8), was adsorbed to carbon-coated grids and negatively stained with uranyl acetate for imaging in the electron microscope. Fields of many similar particles were observed, which suggests that Mediator exists as a discrete entity, as was previously inferred from biochemical studies. A large fraction of the particles appeared to be nearly identical, which is indicative of a preferred orientation on the grid (9).

Department of Structural Biology, Fairchild Building, Stanford University School of Medicine, Stanford, CA 94305, USA.

*Present address: Department of Cell Biology MB 25, The Scripps Research Institute, 10550 North Torrey Pines Road, La Jolla, CA 92037, USA.

†Present address: Institute of Medical Biochemistry, Göteborg University, Medicinaregatan 13, 405 30 Göteborg, Sweden.

‡To whom correspondence should be addressed. E-mail: kornberg@stanford.edu

REPORTS

Images of such particles were aligned and averaged with the use of the SPIDER suite of programs (10, 11). The resulting view of the Mediator structure in projection revealed details to about 40 Å resolution (Fig. 1). The structure measured about 400 Å in height and appeared roughly triangular in shape, with a distinct dense domain at the base.

When Mediator and RNA polymerase II were mixed in equimolar (0.05 μM) amounts, about 75% of the Mediator associated with polymerase to form holoenzyme. Many images of the remaining unassociated Mediator exhibited a partially extended conformation. Three domains, barely distinguishable in the compact form of Mediator found in the absence of polymerase, were linearly arrayed, with variable angles between them (Fig. 2).

Alignment and averaging of holoenzyme images revealed Mediator in a fully extended

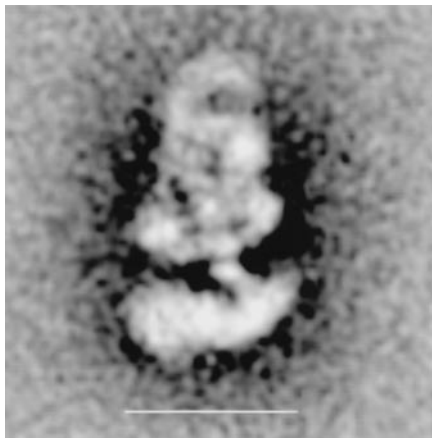


Fig. 1. Yeast Mediator in projection. Images of 54 individual particles were aligned and averaged. Scale bar, 200 Å.

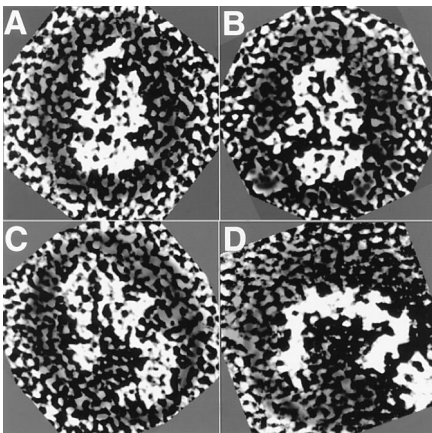
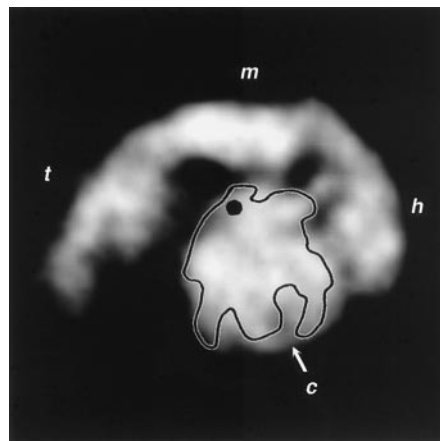


Fig. 2. Contrast-enhanced images of single yeast Mediator particles. Closed and progressively more extended conformations of Mediator (A through D) are shown. Part of an RNA polymerase II molecule is included alongside the Mediator particle in the lower righthand corner of (D). The background around the Mediator particles was partially blocked for ease of viewing.

form (Fig. 3). Mediator was identified as an arc of protein density on the periphery, on the basis of the similarity in appearance and dimensions to the partially extended form (Fig. 2). The three Mediator domains were clearly distinguishable in the holoenzyme, the largest of which is referred to here as the “head,” presumably corresponding to the dense domain at the base of Mediator in the compact form, followed by “middle” and “tail” domains.

The central globular density in the image of the holoenzyme was identified as RNA polymerase II by comparison with images of the polymerase alone and with the three-dimensional (3D) structure of the enzyme, previously determined at 16 Å resolution from two-dimensional (2D) crystals in negative stain (12). A view of the polymerase structure in projection was found, whose outline (dark line in Fig. 3) roughly matched that of the polymerase density in the holoenzyme and that placed the CTD region of the polymerase structure, also known from 2D crystallography (13) (black dot in Fig. 3), adjacent to the Mediator density of the holoenzyme. With the polymerase in this orientation, the CTD contacted the Mediator middle domain. A second contact with Mediator was formed between a region of the polymerase in the vicinity of the DNA-binding channel (arrow



in Fig. 3) and the Mediator head domain. There was no apparent contact between the polymerase and the Mediator tail domain, which was nonetheless well localized, suggesting conformational rigidity of the extended Mediator structure.

As a control, Mediator was mixed with RNA polymerase II lacking a CTD and examined in the electron microscope (14). No holoenzyme was observed, although some Mediator particles appeared to be partially extended. Inasmuch as unfolding only occurred in the presence of polymerase, unfolding in the absence of a CTD was consistent with a second site of Mediator-polymerase interaction. Also, no unfolding was observed upon incubation of Mediator with a CTD peptide, and neither holoenzyme formation nor unfolding of yeast Mediator occurred in the presence of mammalian RNA polymerase II. An activator protein that functions through Mediator, Gal4-VP16, also failed to cause unfolding. Mediator persisted in the compact configuration under a range of solution conditions, except for prolonged incubation at 40°C, which caused the apparent loss of the headpiece from many Mediator particles, and exposure to a pH above 8.5, which caused extensive unfolding, even in the absence of polymerase. Unfolding at elevated pH was re-

Fig. 3. Holoenzyme formed by yeast Mediator and RNA polymerase II in projection. Images of 73 particles were aligned and averaged to calculate the map. Mediator is in an extended conformation, with head (h), middle (m), and tail (t) domains clearly distinguishable. The globular density embraced by Mediator is identified as RNA polymerase II. The outline of a projection of the previously determined polymerase 3D structure is superimposed (dark line), with the point of attachment of the CTD (dark circle) and the location of the DNA-binding channel (c) indicated. This alignment is speculative because of the low (~40 Å) resolution of the holoenzyme map and possible conformational changes of the polymerase upon interaction with Mediator.

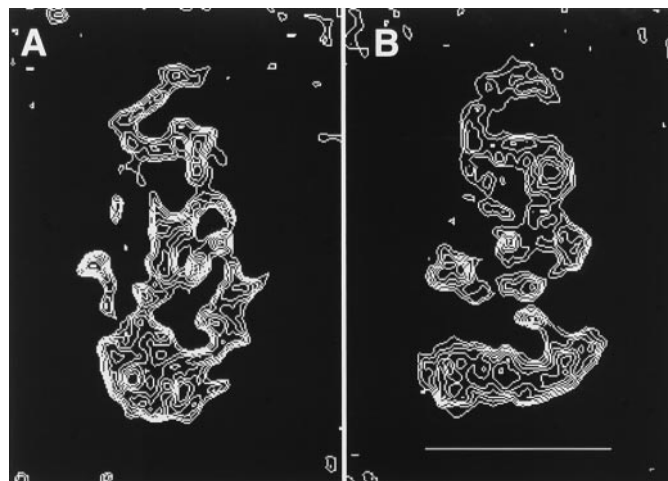


Fig. 4. Murine Mediator in projection (A), compared with its yeast counterpart (B). Images of 66 individual particles, purified from murine hybridoma cells as described (6), were aligned and averaged. The maps are displayed as contour plots to emphasize their main features. Scale bar in (B), 200 Å.

versed by restoration of neutrality, although the refolded Mediator appeared slightly different from the original compact form.

The related murine complex, containing homologs of yeast Mediator subunits (6), appeared similar to yeast Mediator in the electron microscope. Fields of well-defined particles gave evidence of a discrete complex, and selection, alignment, and averaging yielded a view in projection. The murine complex was not only the same size and shape as yeast Mediator but also bore a close resemblance in internal structural detail (Fig. 4). The very occurrence of such a view, deriving from a preferred orientation on the surface of the electron microscope grid, points to a similarity in 3D structure of the two complexes, leading to a similar manner of adsorption to the grid.

The murine complex also underwent a conformational change to an extended form at high pH or in the presence of RNA polymerase II (14). Unfolding was again species specific, occurring only with mammalian but not with yeast RNA polymerase II. The proportion of extended particles was, however, smaller, and the images of holoenzyme were more variable, precluding alignment and averaging. The similarity to yeast holoenzyme was nonetheless apparent from views of individual particles.

Parallel investigation of the murine and yeast complexes was of particular interest because of the apparent differences between them. Although four components of the murine complex are homologous to yeast Mediator subunits, there is as yet no evidence of further homology, with a murine equivalent of the Sin4/Rgr1 repression-activation module being conspicuously lacking (6). The structural similarities noted here point to a correspondence between the two complexes: Both occur in a compact conformation of about the same size and shape and exhibit similar internal structural detail; both unfold to an extended conformation at elevated pH or in the presence of RNA polymerase II; and both interact with polymerase in the extended conformation, forming holoenzymes that are similar in general appearance. Moreover, both complexes include a tail domain, as identified in a preliminary study of yeast Mediator from a *sin4* deletion strain as the Sin4/Rgr1 repression-activation module (15). Thus, the murine complex appears to be a true counterpart of yeast Mediator.

Unfolding of Mediator in the presence of RNA polymerase II may reflect the equilibrium association of the two proteins detected previously by biochemical means (16). Mediator unfolds upon binding polymerase and fails to refold immediately after dissociation. The evidence for at least two sites of interaction with polymerase was unexpected. It was previously thought that the interaction occurred solely through the polymerase CTD. The species specificity of Mediator unfolding, as well as its persistence in the absence of the CTD, provide

evidence for a second site. Apparently both sites are required for a stable interaction.

References and Notes

1. P. M. Flanagan, R. J. Kelleher III, M. H. Sayre, H. Tschochner, R. D. Kornberg, *Nature* **350**, 436 (1991).
2. Y. J. Kim, S. Bjorklund, Y. Li, M. H. Sayre, R. D. Kornberg, *Cell* **77**, 599 (1994).
3. C. M. Thompson, A. J. Koleske, D. M. Chao, R. A. Young, *ibid.* **73**, 1361 (1993).
4. Y. Li *et al.*, *Proc. Natl. Acad. Sci. U.S.A.* **92**, 10864 (1995).
5. L. C. Myers *et al.*, *Genes Dev.* **12**, 45 (1998).
6. Y. W. Jiang *et al.*, *Proc. Natl. Acad. Sci. U.S.A.* **95**, 8538 (1998).
7. L. C. Myers, K. Leuther, D. A. Bushnell, C. M. Gustafsson, R. D. Kornberg, *METHODS: A Companion to Methods in Enzymology* **12**, 212 (1997).
8. Purified Mediator was assayed in reactions reconstituted with essentially pure transcription proteins (7). Maximal transcriptional activation and maximal stimulation of basal transcription were obtained with levels of Mediator that were less than stoichiometric

with core RNA polymerase II, which is indicative of a high percentage of active Mediator molecules.

9. About 85% of the particles were clearly recognizable as belonging to the reported average conformation and orientation. Most of the remaining particles appeared to be distorted but were easily recognized as variants of the average, most likely affected by the sample preparation procedure (adsorption to the grid and negative staining).
10. J. Frank *et al.*, *J. Struct. Biol.* **116**, 190 (1996).
11. The resolution of all average projection maps, calculated by Fourier ring correlation analysis of partial averages (10), was about 40 Å.
12. S. A. Darst, A. M. Edwards, E. W. Kubalek, R. D. Kornberg, *Cell* **66**, 121 (1991).
13. G. D. Meredith *et al.*, *J. Mol. Biol.* **258**, 413 (1996).
14. F. J. Asturias, Y. W. Jiang, L. C. Myers, C. M. Gustafsson, R. D. Kornberg, data not shown.
15. F. J. Asturias *et al.*, unpublished data.
16. J. Q. Svejstrup *et al.*, *Proc. Natl. Acad. Sci. U.S.A.* **94**, 6075 (1997).
17. Supported by NIH grants AI21144 and GM36659 to R.D.K.

5 October 1998; accepted 7 January 1999

Crystallographic Evidence for Preformed Dimers of Erythropoietin Receptor Before Ligand Activation

Oded Livnah,^{1*} Enrico A. Stura,^{1†} Steven A. Middleton,² Dana L. Johnson,² Linda K. Jolliffe,^{2‡} Ian A. Wilson^{1‡}

Erythropoietin receptor (EPOR) is thought to be activated by ligand-induced homodimerization. However, structures of agonist and antagonist peptide complexes of EPOR, as well as an EPO-EPOR complex, have shown that the actual dimer configuration is critical for the biological response and signal efficiency. The crystal structure of the extracellular domain of EPOR in its unliganded form at 2.4 angstrom resolution has revealed a dimer in which the individual membrane-spanning and intracellular domains would be too far apart to permit phosphorylation by JAK2. This unliganded EPOR dimer is formed from self-association of the same key binding site residues that interact with EPO-mimetic peptide and EPO ligands. This model for a preformed dimer on the cell surface provides insights into the organization, activation, and plasticity of recognition of hematopoietic cell surface receptors.

Erythropoietin (EPO) is a glycoprotein hormone that regulates the proliferation, differentiation, and maturation of erythroid cells (1). The EPO receptor (EPOR), a member of the class 1 cytokine receptor superfamily (2), con-

sists of an extracellular ligand-binding domain, a short single-pass transmembrane segment, and a cytoplasmic domain that lacks a kinase region (3). Signaling occurs through the JAK/STAT pathway, where ligand-induced sequential receptor homodimerization (4-6) has been proposed to promote stable association of JAK2 and phosphorylation of JAK2, EPOR, and STAT5 (7). EPOR can also be activated through a point mutation in the extracellular region (EPO binding protein, EBP) that produces a disulfide-linked homodimer (5), by a small percentage of monoclonal antibodies to EPOR (8) and by a set of short EPO-mimetic peptides (9) (EMPs) that are unrelated in sequence to EPO and can be considered minimized hormones (9, 10). The crystal structure of an agonist EMP1-EBP complex (11) revealed a two-

¹Department of Molecular Biology and Skaggs Institute of Chemical Biology, The Scripps Research Institute, 10550 North Torrey Pines Road., La Jolla, CA 92037, USA. ²R. W. Johnson Pharmaceutical Research Institute, Drug Discovery Research, 1000 Route 202, Box 300, Raritan, NJ 08869, USA.

*Present address: Department of Biological Chemistry, Institute of Life Sciences, Wolfson Centre for applied Structural Biology, Hebrew University of Jerusalem, Jerusalem 91904, Israel.

†Present address: Department d'Ingenierie et d'Etude des Proteines, BAT 152 C.E.A./SACLAY, 91191 Gif sur Yvette Cedex, France.

‡ To whom correspondence should be addressed.